

PAPER • OPEN ACCESS

Maximum pulsar mass, equation of state and structure of neutron-star cores

To cite this article: P Haensel and J L Zdunik 2016 *J. Phys.: Conf. Ser.* **665** 012061

View the [article online](#) for updates and enhancements.

Related content

- [Collective excitations in neutron-star crusts](#)
N Chamel, D Page and S Reddy
- [Equations of state](#)
James A Beattie and Walter H Stockmayer
- [Modeling of neutron-star mergers: a review while awaiting gravitational-wave detection](#)
Luca Baiotti

Recent citations

- [Effects of the \$\sigma\$ and Mesons on the Properties of Massive Protoneutron Stars](#)
Xueling Mu *et al.*

Maximum pulsar mass, equation of state and structure of neutron-star cores

P Haensel and JL Zdunik

N. Copernicus Astronomical Center, Polish Academy of Sciences, Bartycka 18, PL-00-716
Warszawa, Poland

E-mail: haensel@camk.edu.pl jlz@camk.edu.pl

Abstract.

The structure of neutron stars is determined by the equation of state of dense matter in their interiors. Brief review of the equation of state from neutron star surface to its center is presented. Recent discovery of two two-solar-mass pulsars puts interesting constraints on the poorly known equation of state of neutron-star cores for densities greater than normal nuclear matter density. Namely, this equation of state has to be stiff enough to yield maximum allowable mass of neutron stars greater than two solar masses. There are many models of neutron stars cores involving exclusively nucleons that satisfy this constraint. However, for neutron-star models based on recent realistic baryon interaction, and allowing for the presence of hyperons, the hyperon softening of the equation of state yields maximum masses significantly lower than two solar masses. Proposed ways out from this "hyperon puzzle" are presented. They require a very fine tuning of parameters of dense hadronic matter and quark matter models. Consequences for the mass-radius relation for neutron stars are illustrated. A summary of the present situation and possible perspectives/challenges, as well as possible observational tests, are given.

1. Introduction

The equation of state (EOS) of neutron stars (NS) is one of their mysteries. For astrophysically interesting masses, $M > M_{\odot}$, and for NS which are older than a year, the effects of temperature, magnetic field, and of rotation, on the NS structure are small [1], and will be neglected here. Then, the structure of NS, and in particular their maximum allowable mass, M_{\max} , is determined by the EOS [1].

To construct models of NS, from the surface (or rather from an atmosphere, which is however typically only a few cm thick) to the star's center, we need the EOS for density from a fraction of g cm^{-3} up to some $5 \times 10^{15} \text{ g cm}^{-3}$. A general overview of theoretical EOSs for NS, from the surface to the center, is given in Sect. 2.

As we stress in Sect. 2, at density larger than 10^6 g cm^{-3} , matter in NS is strongly degenerate, and therefore pressure becomes a function of the density only, $P = P(\rho)$. Up to the normal nuclear density $\rho_0 = 2.7 \times 10^{14} \text{ g cm}^{-3}$, corresponding to the baryon (number) density $n_0 = 0.16 \text{ fm}^{-3}$, the EOS is rather well established [2]. However, for $\rho > \rho_0$ the uncertainty in the EOS increases rapidly with increasing ρ . This uncertainty is reflected in the uncertainty in the theoretical prediction for M_{\max} , which is the *functional* of $P(\rho)$: $M_{\max}[P(\rho)]$. Recent measurements of two pulsar masses yielded values close to $2 M_{\odot}$: $1.97 \pm 0.04 M_{\odot}$ for PSR J1614-2230 [3] and $2.01 \pm 0.04 M_{\odot}$ for PSR J0348+0432 [4], both masses are quoted with



$\pm 1\sigma$ errors. These measurements imply an important constraint on the EOS at $\rho > \rho_0$ and tell us about crucial importance of strong interactions in dense matter (Sect. 3). Still, the uncertainty in the EOS for $4\rho_0 < \rho < 10\rho_0$ - density range which is crucial for M_{\max} - is very large (Sect. 3). It is therefore interesting to consider absolute upper bounds on M_{\max} based on very basic assumptions (Sect. 4). While we expect that NS matter at $\rho_0 < \rho < 2\rho_0$ is composed mostly of neutrons, with a few percent admixture of protons, electrons, and muons, at higher density hyperons or even quark gluon plasma might appear, forming a strangeness carrying NS-core. Possible EOS resulting from various theoretical models are reviewed in Sects. 3-5. The "hyperon puzzle" and possible ways out from it are also mentioned there. The impact of the uncertainty in the EOS ($\rho > \rho_0$) on the mass vs. central density dependence of NS is described in Sect. 7. The NS radius for $M = 1.0 M_\odot - 1.5 M_\odot$ turns out to be sensitive to the presence of a strange central core. We discuss a potential significance of this feature in the context of recent measurements of radii of NS (Sect. 8). Some (tentative) conclusions are formulated in Sect. 9.

2. Overview of (theoretical) EOS for neutron stars

In general theory of relativity (GTR) the matter density is defined as $\rho = \mathcal{E}/c^2$, where \mathcal{E} is total energy density (including rest energy of particles). Baryon density n_b is baryon number (baryon charge) contained in a unit volume. Using elementary thermodynamics we get relation between pressure P and ρ from calculated $\mathcal{E}(n_b)$

$$P(n_b) = n_b^2 d(\mathcal{E}/n_b)/dn_b, \quad \rho(n_b) = \mathcal{E}(n_b)/c^2 \implies P = P(\rho). \quad (1)$$

An example of a theoretically calculated EOS in the density range from $1 \text{ g cm}^{-3} - 10^{16} \text{ g cm}^{-3}$ is shown in Fig. 1, based on [5]. The black curve corresponds to dense matter in full equilibrium and at $T = 0$ (cold catalyzed matter, equivalent to the ground state of the matter, see e.g. [1]). Zero pressure is reached at 8.56 g cm^{-3} , and the ground state of the matter is then a ^{56}Fe crystal [1]. Above 10^4 g cm^{-3} atoms are crushed (full "pressure ionisation") and matter consists of a lattice of nuclei immersed in an electron gas: this is the "outer crust" of NS existing down to the "neutron-drip point" $\rho_{\text{ND}} \sim 4 \times 10^{11} \text{ g cm}^{-3}$ (pressure $P_{\text{ND}} \sim 10^{30} \text{ dyn cm}^{-2}$). Pressure within the outer crust is determined mainly by the contribution of the electron gas. The inner crust of NS, consisting of a crystal lattice of neutron-rich nuclei permeated by a quasi-uniform electron gas and immersed in a neutron gas, extends down to the crust-core (CC) interface, $\rho_{\text{ND}} < \rho < \rho_{\text{CC}}$, with inner crust edge at $\rho_{\text{CC}} \simeq (0.3 - 0.5)\rho_0$ and $P_{\text{CC}} \simeq 10^{33} \text{ dyn cm}^{-2}$; the relative density jump at the crust-core interface is less than one percent [1].

NS are born as very hot objects, with internal temperature exceeding 10^{11} K . However, due to efficient neutrino emission, they cool to less than 10^9 K in a few months. For observed isolated NS ($10^2 - 10^4 \text{ y}$ old) a typical (measured) surface temperature is $\sim 10^6 \text{ K}$; it is expected to be significantly larger $\sim 10^8 \text{ K}$ in the deep interior. As seen in Fig. 1, for observed isolated NS the effect of T on the EOS at $\rho > 10^4 \text{ g cm}^{-3}$ can be safely neglected, because matter is strongly degenerate there.

Actually, the structure of the crust accreted by a NS in a close binary is expected to be very different from the ground-state one [2]. However, the difference in the EOS of the ground-state and accreted crust are significant only in the inner crust in the density range $5 \times 10^{11} - 5 \times 10^{12} \text{ g cm}^{-3}$, where the accreted crust is stiffer [2]. The effect of this stiffening due to accretion on M_{\max} is negligibly small.

For sub-nuclear density ($\rho < \rho_0$) the EOS can be quite reliably calculated, because: (1) matter involves nucleons only, and nuclear forces are tested in terrestrial nuclear physics; (2) in this density range the many-body theories of nuclear matter are well tested in nuclear physics; (3) theoretical calculations of the EOS of pure neutron matter for $\rho < \rho_0$ are quite precise, so that in this limit the EOS is also under control. Unfortunately, the (outermost) sub-nuclear

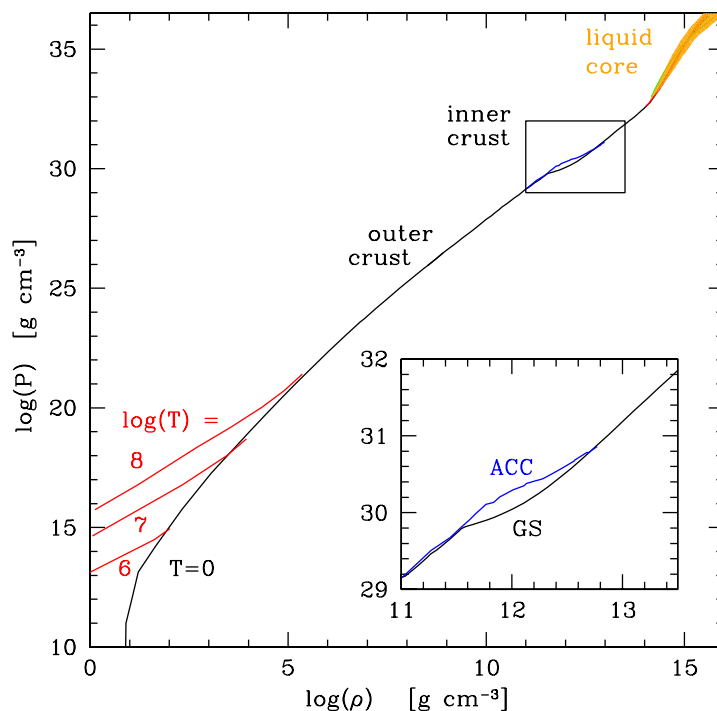


Figure 1. (Color online) An example of the EOS of NS matter from the surface to the center. Based mainly on [5] and [22]. Black line: ground state of dense matter, $T = 0$. Zoomed rectangle: EOS of the inner crust. Blue line - accreted crust, black line - ground state crust [22]. EOS of the liquid core at $\rho > \rho_0$ is uncertain, and the uncertainty grows with increasing ρ . This is visualized by a quasi-triangular colored region. Finite T effect on the EOS of the ^{56}Fe envelope of NS are visible in the bottom-left corner. For $\rho > 10^6 \text{ g cm}^{-3}$ the ^{56}Fe plasma is strongly degenerate even at 10^8 K . Effect of melting of the crust on the EOS for $\rho > 10^6 \text{ g cm}^{-3}$ is so small that it cannot be seen [1].

density layer contains only (1 – 3)% of NS mass for $M = 1.4 M_\odot$ and less than one percent at $M = M_{\text{max}} > 2 M_\odot$.

For $\rho > \rho_0$ uncertainty in the EOS, growing rapidly with increasing ρ , reflects our lack of knowledge of strong interactions in dense matter (e.g., three- and four-body forces) and deficiencies and uncontrolled approximations of the many-body theories. This is visualized by a colored quasi-triangular sector of the high-density EOS in Fig. 1.

3. Uncertainties in the EOS($\rho > \rho_0$)

First calculation of M_{max} within the general theory of relativity (GTR) was based on an EOS of a free Fermi gas (FFG) of neutrons [6] and yielded $M_{\text{max}}[\text{FFG}] = 0.7 M_\odot$. The recent measurement of $2 M_\odot$ masses of two pulsars is an observational (experimental) proof of a dominating rôle of (repulsive) strong interactions in the EOS of NS, because

$$M_{\text{max}}^{(\text{obs})} / M_{\text{max}}[\text{FFG}] > 2.8. \quad (2)$$

A strict condition $M_{\text{max}}[\text{EOS}] > 2 M_\odot$ restricts very strongly a set of acceptable theoretical EOS for $\rho > \rho_0$. These EOS have to be much stiffer than the FFG one. On the other hand, the EOS should respect a fundamental constraint stemming from the special theory of relativity:

the speed of sound must not exceed c ,

$$v_s = (dP/d\rho)^{1/2} \leq c . \quad (3)$$

The above condition is usually interpreted as equivalent to a more fundamental condition of *causality* (for a detailed discussion, see [7]). One can easily construct so called *causal limit* (CL) equation of state, matched smoothly to another EOS at the point (ρ_m, P_m) and which is maximally stiff, $v_s = c$ for larger density,

$$P^{(\text{CL})} = P_m + (\rho - \rho_m)c^2 \text{ for } \rho > \rho_m . \quad (4)$$

A true EOS($\rho > \rho_0$) is a line in the $P - \rho$ plane. Our ignorance implies that there are many proposed theoretical EOS satisfying necessary conditions $\{M_{\text{max}}[\text{EOS}] > 2 M_{\odot}\} \wedge \{v_s \leq c\}$ and used as "the EOS". They span over a characteristic quasi-triangular region in the $P - \rho$ plane, similar to that shown in the left panel of Fig. 2.

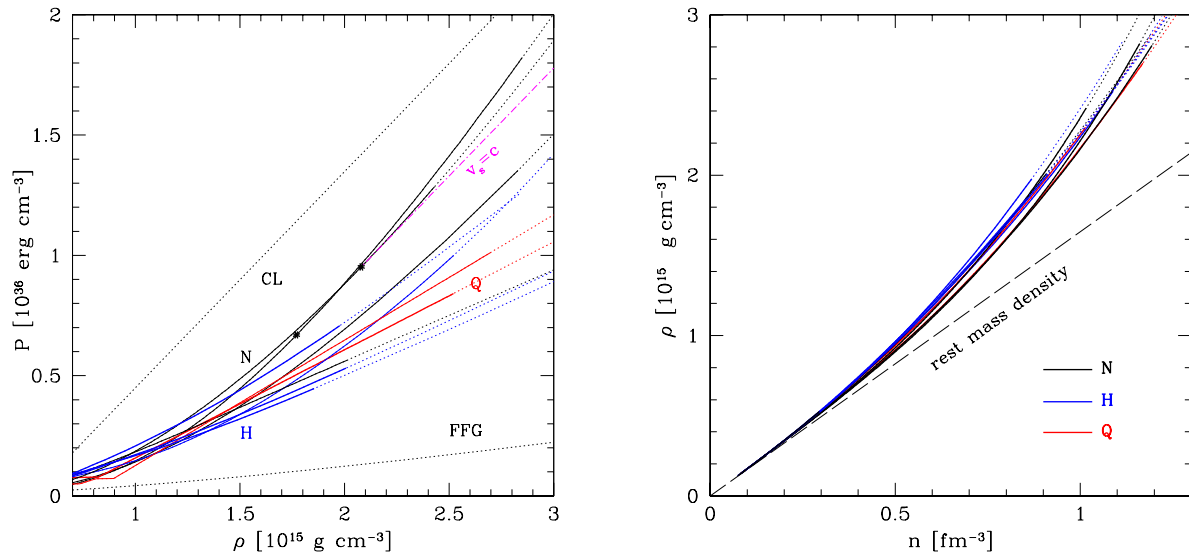


Figure 2. (Color online) **Left panel:** A set of the high-density EOS from the families N (EOS.N), H (EOS.NH), and Q (EOS.BQ), in the $P - \rho$ plane, for $\rho > 7 \times 10^{14} \text{ g cm}^{-3}$. (a) Dotted line CL: causal limit EOS of the form $P = (\rho - \rho_1)c^2$, where $\rho_1 = 5 \times 10^{14} \text{ g cm}^{-3}$. It crosses each of the considered EOS at some point (ρ_m, P_m) such that $\rho_m = \rho_1 + P_m/c^2$; (b) Dotted line FFG: EOS of a free Fermi gas of neutrons. (c) Asterisk on an EOS indicates the point beyond which EOS is non-causal ($v_s > c$); (d) We matched to the APR EOS a CL.EOS starting at the asterisk and denoted by a dot-dash line; the segment of the APR EOS above dot-dash line has to be rejected as non-causal; (e) The constant pressure segments in the quark part of the EOS.BQ correspond to the 1st order phase transitions, associated with a density jump.

Right panel: Mass density $\rho = \mathcal{E}/c^2$ vs. baryon density n_b for NS matter. Relation $\rho = \rho(n_b)$ deviates from linearity for $n_b > 0.3 \text{ fm}^{-3}$. Nonlinearity grows with increasing n_b and is EOS-dependent. For $n_b < 0.2 \text{ fm}^{-3}$ linear approximation $\rho \approx n_b m_n$ (where m_n is neutron mass) is valid.

4. Absolute upper bounds on M_{max}

In view of the uncertainties in the theoretical EOS at supra-nuclear densities, it is of interest to derive an absolute upper bound on M_{max} , based on a fundamental physical argument. It is clear that CL.EOS, Eq. (4), will maximize M_{max} for NS models with "known envelope" $\rho < \rho_m$

and an "unknown core" $\rho > \rho_m$ ". For massive NS with mass close to $2 M_\odot$, the mass fraction contained in the outer layer with $\rho < \rho_m$ is negligibly small. Then, a following inequality holds (see [1] and references therein):

$$M_{\max} \leq M_{\max}^{(\text{CL})} = 3.0 \left(\frac{5 \times 10^{14} \text{ g cm}^{-3}}{\rho_m} \right)^{\frac{1}{2}} M_\odot, \quad (5)$$

where $M_{\max}^{(\text{CL})}$ is a maximum allowable mass for NS with CL.EOS within the core $\rho > \rho_m$. The formula for $M_{\max}^{(\text{CL})}$ is quite precise provided $\rho_m \leq 5 \times 10^{14} \text{ g cm}^{-3}$ [1]. The most conservative upper bound is $\rho_m = \rho_0 \implies M_{\max}^{(\text{CL})} = 4.1 M_\odot$. Therefore the true value of M_{\max} fulfills inequality $2.0 < M_{\max}/M_\odot < 4.1$.

5. Structure of dense matter and fundamental aspects of the EOS

As we will see in the next sections, a suitable unit for the density in NS cores is $10^{15} \text{ g cm}^{-3}$, and the relevant density is written as $\rho_{15} \equiv \rho/(10^{15} \text{ g cm}^{-3})$. The density range in NS cores is $0.3 < \rho_{15} < 3$, and in order to (theoretically) study NS we need $P(\rho)$ in this interval of matter density.

5.1. Nucleon cores: EOS.N

At $\rho = \rho_0$ NS core consists of nuclear matter (some 95% of neutrons, 5% of protons), and electrons that neutralize proton electric charge [1]. It is expected that for $\rho_0 < \rho \lesssim 2\rho_0$ (outer NS core) nucleons are the only baryons present in NS matter. The "minimal" EOS of NS matter consisting of nucleons and leptons will be denoted as EOS.N. It is based on the 2-body nucleon forces (2BF) fitting a few thousand of data on nucleon-nucleon scattering and the properties of ${}^2\text{H}$ \boxed{np} . Moreover, we are forced to consider three-body nucleon forces (3BF), which have to reproduce the properties of ${}^3\text{H}$ \boxed{nnp} , ${}^3\text{He}$ \boxed{ppn} , ${}^4\text{He}$ \boxed{nnpp} , and the semi-empirical parameters of nuclear matter at saturation.

Numerous many-body calculations of EOS.N starting from 2BF+3BF and performed within the quantum many-body theories of dense matter yield $M_{\max} > 2 M_\odot$ (see, e.g. [8]).

5.2. Nucleon-hyperon cores: EOS.NH

Since more than fifty years it is believed that above some supranuclear density purely nucleon NS cores become unstable with respect to weak-interaction processes and that hyperons might replace the most energetic nucleons due to the strangeness-changing reactions. Consequently, NS with sufficiently high central density could have strangeness carrying (strange) cores consisting of nucleon-hyperon (hypernuclear) matter; their EOS is denoted by EOS.NH. As nucleons and hyperons are baryons, we will sometimes replace NH by B(baryons). The calculation of EOS.NH necessitates models of nucleon-hyperon and hyperon-hyperon forces. The nucleon-hyperon interaction is obtained from the analyses of hypernuclei and Σ^- -atoms, while hyperon-hyperon forces are estimated studying double $\Lambda\Lambda$ hypernuclei. The data on the hyperon interactions are scarce, or even nonexistent in many hyperon-nucleon and hyperon-hyperon channels, and therefore approximate symmetries of strong interactions have to be widely used to get a hypernuclear interaction. Another painful problem is our ignorance concerning the three-body forces involving hyperons.

Appearance of the hyperons leads to a significant softening of the EOS.NH compared to EOS.N where the hyperons are suppressed, because hyperons that replace the most energetic nucleons, are more massive than nucleons and move slowly, because they have small Fermi momenta (densities). Actually, for baryonic force models which are consistent with available nuclear and hypernuclear data, a few existing Brueckner-Bethe-Goldstone theory calculations

yield $M_{\max}[\text{EOS.NH}] \lesssim 1.5 M_{\odot}$ ([9] and references therein). This is in dramatic conflict with observation of $2 M_{\odot}$ pulsars: the "hyperon puzzle". One can try to escape from it via a fine tuning of dense matter model (Sect. 6).

Before reviewing proposed "fine tuning" procedures, we will review some fundamental aspects of the structure of dense matter in NS.

5.3. EOS and QCD

According to the modern theory of strong interactions, the Quantum Chromodynamics (QCD), baryons are confined states of three quarks. Only three lightest quarks are involved in terrestrial nuclear and hypernuclear physics. We are dealing with nucleons and nuclei composed of non-strange u and d quarks, and hyperons and hypernuclei, which additionally involve s quark of strangeness -1.

Many-body theory of nuclear and hypernuclear matter tested in low-energy nuclear and hypernuclear physics (i.e., for $\rho \lesssim \rho_0$) does not consider the quark degrees of freedom. Instead, it refers to "effective matter constituents": baryons \boxed{udd} , \boxed{uds} ... In this "effective theory" nuclear forces result from exchange of (virtual) mesons $\boxed{\bar{q}q}$. The effective theory is very successful in low-energy nuclear physics. However, can it be successfully extrapolated up to $10\rho_0$? We have to ask a basic question: how far this effective theory of hadrons+leptons can be used in dense cold matter?

There are two remarkable features of the QCD: confinement of quarks and asymptotic freedom. QCD predicts also a deconfinement of quarks. Namely, there exists a finite density ρ_{dec} such that for $\rho \gtrsim \rho_{\text{dec}}$ cold electrically neutral matter becomes a plasma of quarks interacting via exchange of gluons, maybe with a small admixture of electrons. Unfortunately, both the value of ρ_{dec} and the EOS for $\rho > \rho_{\text{dec}}$ are very difficult to calculate: the many-particle system under consideration is a strongly-interacting quark-gluon plasma.

QCD predicts a very important property of the quark-gluon plasma (QGP). For the mean kinetic energy of quarks in QGP (resulting from the Fermi statistics of quarks) $\gg \Lambda_{\text{QCD}} \sim 1000$ MeV, the EOS is simply $P \simeq \frac{1}{3}\rho c^2$ (EOS of an ultra-relativistic Fermi gas)[10]. This is the consequence of the Asymptotic Freedom of the QCD.

The value of Λ_{QCD} indicates that the region where the Asymptotic Freedom prevails (the region of simplicity - "Asymptopia") is reached for $\rho > 10^{18}$ g cm⁻³ - far larger than maximum density reached at the center of most massive neutron stars. The maximum density reached in NS does not exceed 5×10^{15} g cm⁻³. This implies that only the least massive quarks u , d , s are relevant for NS (see [1]).

6. $2M_{\odot}$ pulsars with strange neutron-star cores and necessity of a fine tuning of the EOS

It has been shown by many authors that NH cores in $2 M_{\odot}$ stars can exist only for very special models of dense hadronic matter. They are all constructed within the relativistic mean-field (RMF) theory of hadronic matter. Additionally, they have specific features leading to a required EOS.NH. First "fine tuned feature" is a strong high-density repulsion acting only between hyperons, and generated by the exchange of the hidden-strangeness $\phi \boxed{s\bar{s}}$ mesons (see, e.g., [11, 12, 13, 14], and other papers). A second "fine tuned feature" is a sufficiently strong breaking of the SU(6) symmetry in the hyperon-meson coupling constants [15].

Strangeness is associated with s quark, either confined into hyperons or moving in a (deconfined) quark plasma. A stiff superconducting quark core instead of hyperon core (such stars are called "hybrid stars" because they have baryon (B) and quark-matter (Q) components) could allow for $M_{\max} > 2 M_{\odot}$ (e.g., [16, 17, 18, 14, 19]). However, necessary conditions on the baryon - quark-matter phase transition (B \rightarrow Q), leading to EOS.BQ respecting $M_{\max} > 2 M_{\odot}$,

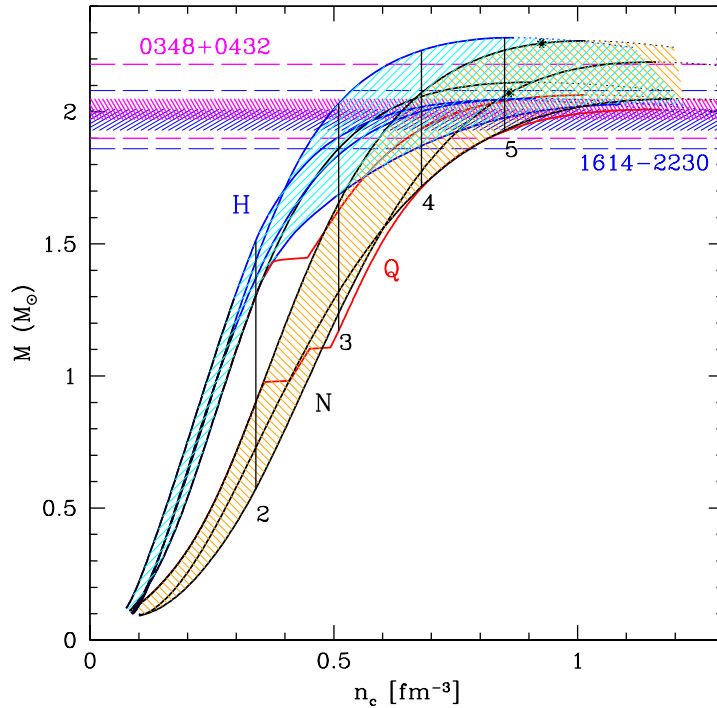


Figure 3. (Color online) Gravitational mass M vs. central baryon density n_c for non-rotating NS models based on the EOS.N (black lines - N family), EOS.NH (blue lines - H family), EOS.BQ (red lines - Q family of hybrid stars). Solid lines: stable NS configurations. Dotted lines: configurations unstable with respect to small radial perturbations. The sign * on a line indicates that $v_s = c$ at the center of this configuration. Configurations to the right of * have $v_s > c$ cores, within which causality is violated. Vertical lines crossing the $M(n_c)$ lines indicate configurations with $n_c/n_0 = 2, 3, \dots$

are very strong. First, the density at which first-order phase transition to quark phase occurs should be similar to the threshold density for hyperons, $\sim 2\rho_0 - 3\rho_0$. Second, the relative density jump at the baryon-quark matter phase transition should be below 30%. Third, quark matter should be sufficiently stiff, which can be expressed as a condition on the sound speed in quark plasma, $v_s/c \simeq 0.8 - 0.9$. Fourth, the pairing in the color-superconducting phase should be strong (energy gap $\sim 50 - 100$ MeV), in order to make the Q-phase thermodynamically stable. All in all, this means a "fine tuning" of the quark-matter phase and of the $B \rightarrow Q$ (1-st order) phase transition.

7. Families of neutron stars

7.1. Two densities: n_b and ρ

When investigating the EOS of NS matter, we have to consider two distinct densities, $\rho = \mathcal{E}/c^2$ and n_b (Sect. 2). While ρ is the relevant quantity for the GTR calculations of the NS structure, it is n_b that leads to a correct evaluation of an average distance between baryons (treated as point-like objects), $r_{bb} \propto n_b^{-1/3}$. Therefore, knowing n_b , we can compare an actual r_{bb} with average distance between nucleons in nuclear matter at normal nuclear density, r_0 , getting $r_{bb}/r_0 = (n_0/n_b)^{1/3}$.

At subnuclear densities, ρ of NS matter can be very well approximated by $n_b m_n$, where m_n is neutron rest mass. However, at supranuclear densities ρ grows nonlinearly with n_b . This

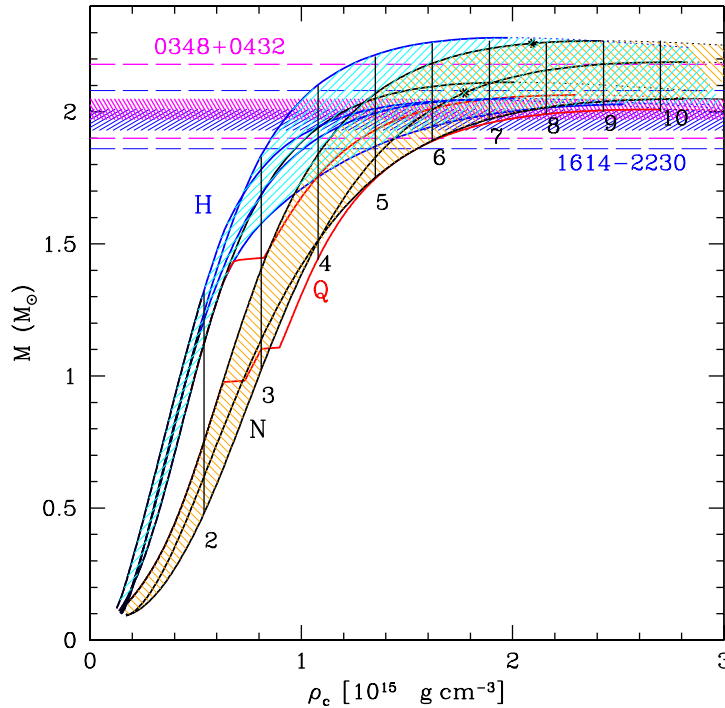


Figure 4. (Color online) Same as for Fig. 3, but with n_c replaced by ρ_c .

nonlinear dependence, as shown in the right panel of Fig. 2, is model dependent.

7.2. Two parametrizations: $M(\rho_c)$ and $M(n_c)$

We restrict to EOS.N, EOS.NH, and EOS.BQ that give $M_{\max} > 2.0 M_{\odot}$. There are several lessons stemming from Fig. 3. First, central density in a $2 M_{\odot}$ NS is typically $n_c/n_0 = 4 - 5$, so that at the star's center $r_{\text{bb}}/r_0 \approx 0.59$. Second, the N segment of EOS.NH corresponding to $n_0 < n_b < 2n_0$ is so much stiffer than the similar segment of EOS.N, that $M^{(\text{NH})}(2n_0) \approx 2 M^{(\text{N})}(2n_0)$. Therefore, in order to yield $M_{\max} > 2.0 M_{\odot}$ in spite of the H-softening, the supranuclear (nucleon) segment $n_0 < n_b < 2n_0$ of EOS.NH has to be very stiff. The fine-tuned H family of $M(n_c)$ curves is, for $0.5 M_{\odot} < M < 1.5 M_{\odot}$, well separated from the N-family and lies above it. This is a well defined result, but n_c is not a measurable quantity, unfortunately.

For the hybrid stars belonging to the Q family the situation is different from that for the N and H families. In view of the n_c and ρ_c jumps associated with 1st order B \rightarrow Q phase transition (or even two jumps, connected with different color-superconducting states, see [18] and the caption to Fig. 3), the $M(n_c)$ curve can cross the gap between the N and H families. This is due to a density jump in a 1st order B \rightarrow Q phase transition combined with an extreme stiffness of the Q-phase, "fine-tuned properties" that still allows the hybrid stars to reach $M_{\max} > 2 M_{\odot}$.

The $M(\rho_c)$ curves are displayed in Fig. 4. The gap between N and H families for $0.5 M_{\odot} < M < 1.5 M_{\odot}$ exists, and some other features are also similar to those of the $M(n_c)$ curves. The asterisks * signal the breaking of the $v_s \leq c$ condition.

Vertical lines crossing the $M(\rho_c)$ curves indicate $\rho_c/\rho_0 = 2, 3, \dots$. One notices that ρ_c/ρ_0 in $2 M_{\odot}$ stars can be as high as 6 - 7, significantly larger than the corresponding values of n_c/n_0 . For the M_{\max} configurations the difference is even larger. However, let us remind that it is n_c and not ρ_c that determines the mean inter-baryon distance at the star's center.

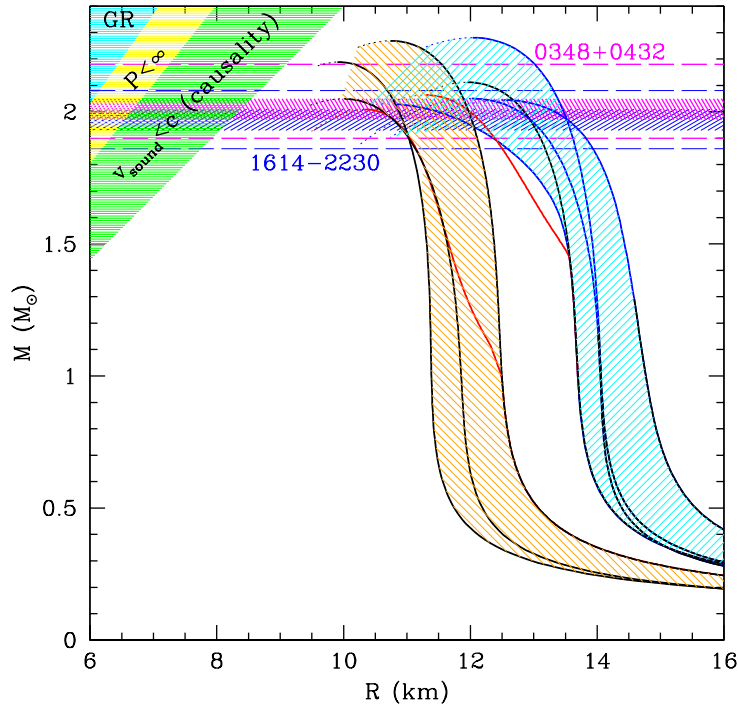


Figure 5. (Color online) Gravitational mass M vs. circumferential radius R for non-rotating NS models. Upper-left corner: (a) blue: excluded by the GTR because $R < 2GM/c^2$; (b) yellow: excluded due to $(\text{GTR}) \wedge (P_c < \infty)$; (c) green: excluded due to $(\text{GTR}) \wedge (v_s < c)$. Otherwise notation as in Figs. 3,4.

8. Hyperon cores and neutron-star radii

The circumferential radius R is an important measurable global parameter of a NS. It can be extracted in the process of analysis of the spectra of the X-ray radiation from the NS atmosphere, provided we know the distance to the star (for a recent review of attempts to measure R see [20], see also [21]). It should be stressed, that due to the GTR effects (spacetime curvature), the value of M has to be involved in the process of determining R , even in a simplest case of non-rotating and non-magnetized NS. Inclusion of rotation and magnetic field strongly complicates the analysis of the collected X-ray spectra.

In Fig. 5 we show the $M(R)$ curves for the N, H, and Q families of NS. One notices a sizable R -gap, ~ 1.5 km, between the N and H families of NS, for $0.5 < M/M_\odot < 1.5$. This is an important feature, with interesting consequences. Notice that the R -gap does not exist for $M \approx 2 M_\odot$.

As we mentioned in Sect. 2, the EOS of NS-crust depends on the crust formation scenario. Namely, an accreted crust (ACC) has a significantly stiffer EOS.ACC than the ground-state one, EOS.GS, for $5 \times 10^{11} \text{ g cm}^{-3} < \rho < 5 \times 10^{12} \text{ g cm}^{-3}$. However, the effects of the difference between EOS.ACC and EOS.ACC for the same NS-core and $M > 1 M_\odot$ is small. For example, for $M = 1.4 M_\odot$, $R_{\text{ACC}} - R_{\text{GS}} \approx 100 \text{ m}$ [22]. This difference decreases with increasing M .

9. Conclusion

In this final section we will focus on the features of the EOS, that stem from the $M_{\text{max}} > 2 M_\odot$ condition. As we have seen, not only an additional repulsion acting between the hyperons has to be included in the hyperon core (due to ϕ -meson exchange or a sufficiently strong SU(6)

symmetry breaking), but also the EOS *before* the hyperonization has to be very stiff. This gives us a "way out" from the "hyperon puzzle", but as for now, it cannot be called a "solution". For the time being, the "way out" is limited only to a class of the Relativistic Mean Field models of hadronic matter (unsuccessful trials of a sufficient stiffening of EOS.NH in the Brueckner-Bethe-Goldstone theory are reviewed in [23]). However, if we accept the RMF models of the EOS.NH, respecting $M_{\max} > 2 M_{\odot}$, then we find interesting properties of NS that could be confronted with measurements of M and R . Namely, for the M -range $1.0 - 1.5 M_{\odot}$ the stars with hyperon cores need have $R > 13$ km. Best realistic EOS of purely nucleon NS gives $R < 12$ km. Recent analysis in [20] leads to *lower bound* $R > 14$ km of NS with $M < 2.3 M_{\odot}$ in 4U 1724-307 X-ray burster. This lower bound of [20] is valid at 90% confidence level, independently of chemical composition of the NS atmosphere. Of course, measuring a radius of NS is a very complicated task (see a critical review of measurements of radii of different NS by other authors, given in [20]). Clearly, measuring R of a NS is a challenge, but as we tried to show it also gives a hope of unveiling the EOS of NS cores.

Acknowledgments

This work was partially supported by the Polish NCN grants no. 2011/01/B/ST9/04838 and 2014/13/B/ST9/02621.

Note Added in Proof

During two years that elapsed since the submission of our article to the NPA6 Conference Proceedings many papers, relevant to the topic of the present article, were published. In this Note we briefly mention some of them. Fourteen RMF EOS.NH allowing for the hyperon cores and $M_{\max} > 2 M_{\odot}$ were considered in [24], where overpressure of these EOS at n_0 compared to the value obtained in [21], correlated with large value of $R_{1.4}$ (radius of neutron star of mass $1.4 M_{\odot}$) was pointed out. First EOS.NH based on the G-matrix approach yielding $M_{\max} > 2 M_{\odot}$ and $R_{1.4} > 13.5$ km was calculated [25]. An EOS.NH based on the RMF model with hadron masses and coupling constants depending on the scalar field, yielding $M_{\max} > 2 M_{\odot}$ and $R_{1.4} = 12$ km was obtained in [26]. However, even at maximum mass the strangeness per baryon was smaller than one percent. New measurements of the radii of neutron stars were carried out [27, 28, 29, 30, 31]. The lower bound of 14 km found in [20] has been very recently revised and decreased to 10.5 km in a very recent preprint [32]. Generally, controversies and uncertainties associated with measured values of R are still too large to allow for a reliable determination of the true EOS of neutron stars.

References

- [1] Haensel, P., Potekhin, A.Y., Yakovlev, D.G. 2007, Neutron Stars 1. Equation of State and Structure (New York, Springer)
- [2] Chamel N., Haensel P. 2008, Living Reviews in Relativity, vol.11, no.10
- [3] Demorest P.B., et al., 2010, Nature 467, 1081
- [4] Antoniadis J. et al. 2013, Science 340, 448
- [5] Haensel P., Potekhin A.Y. 2004, A&A 428, 191
- [6] Oppenheimer J.R., Volkoff G.M. 1939, Phys. Rev. 54, 540
- [7] Fayngold M. 2008, Special Relativity and How it Works, Wiley VCH
- [8] Chamel N., Haensel P., Zdunik J.L., Fantina A.F. 2013, Int. J. Mod. Phys. E22, 1330018
- [9] Schulze H.-J., Rijken T. 2011, Phys. Rev. C 84, 035801
- [10] Collins J.C., Perry M.J. 1975, Phys.Rev.Lett. 34, 1353
- [11] Dexheimer V., Schramm, S. 2008, ApJ, 683, 943
- [12] Bednarek I., Haensel P., Zdunik J.L., Bejger M., Mańka R., 2012, A&A 543, A157
- [13] Weissenborn S., Chatterjee D., Schaeffner-Bielich J. 2012, arXiv:1112.0234
- [14] Bonanno, L., Sedrakian, A. 2012, A&A 539, A16
- [15] Weissenborn S., Chatterjee D., Schaeffner-Bielich J. 2012, Nucl.Phys.A 881, 62
- [16] Blaschke D., Klähn T., Lastowiecki R., Sandin F. 2010, J. Phys. G: Nucl. Part. Phys 37, 094063

- [17] Weissenborn S., Sagert I., Pagliara G., Hempel M., Schaeffner-Bielich J. 2011, *ApJ Lett.* 740, L14
- [18] Zdunik J.L., Haensel P. 2013, *A&A* 551, A61
- [19] Colucci G., Sedrakian, A. 2013, *Phys. Rev. C* 87, 055806
- [20] Suleimanov V., Poutanen J., Revnivtsev M., Werner K. 2011, *ApJ*, 742, 122
- [21] Hebeler K., Lattimer J.M., Pethick C.J., Schwenk A. 2013, *Apj* 773, 11
- [22] Zdunik J.L., Haensel P. 2011, *A&A* 530, A137
- [23] Vidana, I., Logoteta, D., Providencia, C., Bombaci, I., 2011, *Europhys. Lett.*, 94, 11002
- [24] Fortin, M., Zdunik, J.L., Haensel, P., Bejger, M., 2015, *A&A*, 576, A68
- [25] Yamamoto, Y., Furumoto, T., Yasutake, N., Rijken, T.A., 2014, *Phys. Rev. C*, 90, 045805
- [26] Maslov, K.A., Kolomeitsev, E.E., Voskresensky, D.N., 2015, *Phys. Lett. B*, 748, 369
- [27] Bogdanov, S., 2013, *ApJ*, 762, 96
- [28] Guver, T., Ozel, F., 2013, *ApJ*, 765, L1
- [29] Poutanen, J., Nattila, J., Kajava, J.J.E., 2014, *MNRAS*, 442, 3777
- [30] Guillot, S., Servillat, M., Webb, N.A., Rutledge, R.E., 2013, *ApJ*, 772, 7
- [31] Lattimer, J.M., Steiner, A., 2014, *ApJ*, 784, 123
- [32] Nattila, J., Steiner, A.W., Kajava, J.J.E., Suleimanov, V.F., Poutanen, J., 2015, arXiv:1509.06561v1[astro-ph.HE] 22 Sep 2015